*Korean J. Chem. Eng.*, 32(2), 230-238 (2015)
DOI: 10.1007/s11814-014-0217-x

pISSN: 0256-1115
eISSN: 1975-7220

# Oxidation of formaldehyde, carbon monoxide and methanol over manganese-cerium-aluminum oxides supported on cordierite monoliths

**Soo Wan Jeon*, Jung Eun Lee*, Jung Kyu Park**, and Sang Hwan Kim*,†**

*Department of Chemical Engineering, Konkuk University, Seoul 143-701, Korea
**Department of Mechanical Engineering, Konkuk University, Seoul 143-701, Korea
(*Received 1 March 2014 • accepted 30 July 2014*)

**Abstract**−Catalytic oxidation of formaldehyde, carbon monoxide, and methanol over cordierite-supported manganese-cerium-aluminum mixed oxides was investigated in a laboratory reactor. The activities of base metal oxides (BMO) comprising 27% $MnO_2$, 21% $CeO_2$, and 52% $Al_2O_3$ supported on cordierite monoliths calcined at 1,000 °C for 3 h in air dropped very rapidly due to the migration of mobile silicon dioxide ($SiO_2$) from the cordierite to the base metal oxides to react with or physically block the active catalysts. To immobilize migrating $SiO_2$, barrier coats composed of alkali metal (Ba, Sr, Ca, Mg) oxides and alumina were applied to the cordierite prior to coating with active base metal oxides. The base metal oxides supported on cordierite monoliths pretreated with $BaO$-$Al_2O_3$ barrier coats and calcined at 1,000 °C for 3 h in air, initiated the oxidation of HCHO, CO, and $CH_3OH$ at 150, 220, and 170 °C, respectively. These catalysts turned out to be more effective for the formaldehyde oxidation than 0.5% $Pt/Al_2O_3$ precious metal catalysts. Carbon monoxide and methanol oxidation conversions were comparable. The incorporation of small amount of palladium (0.147 wt%) to base metal oxides supported on cordierite monoliths pretreated with $BaO$-$Al_2O_3$ barrier coats, showed the superiority for HCHO, CO, and $CH_3OH$ oxidation to 0.5% $Pt/Al_2O_3$ precious metal catalysts. The temperatures of 50% conversion of formaldehyde, carbon monoxide and methanol were 70 °C lower over base metal oxides catalysts than over precious metal catalysts.

Keywords: Formaldehyde, Methanol, Base Metal Oxide, Cordierite, Barrier Coat

## INTRODUCTION

Catalytic oxidation can effectively remove formaldehyde, carbon monoxide, and methanol from the exhaust of methanol-fueled vehicles. The exhaust of methanol-fueled vehicles differs from that of gasoline-fueled vehicles principally by the composition of the organic constituents. Formaldehyde, carbon monoxide, and methanol concentrations emitted from methanol-fueled vehicles are much higher than those emitted from gasoline-fueled vehicles [1]. The negligible emission of sulfur compounds from methanol-fueled vehicles represents another significant difference between methanol and gasoline exhaust.

These differences in composition of methanol- and gasoline-vehicle exhaust raise the possibility that the optimum catalyst for methanol-vehicle exhaust may differ from that for gasoline-vehicle exhaust. To explore this possibility, laboratory oxidation experiments were conducted with a series of catalysts containing group 7 (Mn), 8 (Ru), 9 (Rh), 10 (Ni, Pd, Pt), and 11 (Cu, Ag, Au) metals as the active components [2-12]. Most of metals were dispersed on $\gamma$-$Al_2O_3$ beads. Partial oxidation and dehydrogenation of methanol to formaldehyde were anticipated to be a problem with some catalysts as suggested in the literature [13,14]. The activities and selectivities of the catalysts were examined primarily as a function of temperature. Particular attention was given to the relative activities and formaldehyde selectivities during low-temperature oxidation since methanol-fueled vehicles generate high emission rates of formaldehyde during cold-start and warm-up.

Early in 1984, McCabe and McCready [15] studied formaldehyde oxidation on a Pt wire and found that the kinetics of the Pt-catalyzed oxidation of formaldehyde is similar to carbon monoxide oxidation kinetics. McCabe and Mitchell [16-18] employed a prereactor to produce formaldehyde by the partial oxidation of methanol to simulate vehicle exhaust in which methanol and carbon monoxide were also present. They found that the catalysts containing Pt and Pd supported on $\gamma$-$Al_2O_3$ beads oxidized methanol very rapidly in the absence of CO, but in the presence of CO the methanol oxidation activity was strongly deactivated. In contrast to the Pt and Pd catalysts, methanol oxidation over the Ag and Cu-Cr catalysts supported on $\gamma$-$Al_2O_3$ beads, is virtually unaffected by the presence of CO. Consequently, although the Ag and Cu-Cr catalysts are much less active than the Pt and Pd catalysts in the absence of CO, their low-temperature activities are comparable to or better than those of the Pt and Pd catalysts in the presence of CO. They also reported that the most unusual behavior was observed with the Pd catalysts, which showed local minima in the HCHO conversion versus temperature profiles.

Foster and Masel [19] investigated the kinetics of formaldehyde oxidation and found that the oxidation rate showed a complicated dependence on the feed composition. The rate was enhanced by adding the $CO_2$ in the feed. Imamura et al. [20,21] studied the formaldehyde oxidation over $CeO_2$-supported Ru and Ag precious metal catalysts using aqueous formaldehyde containing methanol as a

†To whom correspondence should be addressed.
E-mail: sanghkim@konkuk.ac.kr

stabilizer in the feed. Silver-cerium composite oxide was active for low temperature oxidative decomposition of formaldehyde. The surface oxygen of this composite catalyst was removed more easily than that on single component $Ag_2O$ or $CeO_2$, which also seemed to contribute to the high activity of this catalyst. IR analysis revealed that the formaldehyde decomposed both on silver-cerium composite catalyst and $CeO_2$ in the presence of oxygen.

Mao and Vannice [22] investigated formaldehyde oxidation over Ag catalysts dispersed on $\alpha$-$Al_2O_3$ and $SiO_2$. They found that at 200 °C the reaction orders were near 0.3 for both HCHO and $O_2$. Arias' group [23,24] studied the formaldehyde and methanol oxidation over Mn and Pd-Mn catalysts supported on $\gamma$-$Al_2O_3$. They showed that alumina-supported manganese catalysts with manganese loadings ranging from 3.9 to 18.2 wt% achieved total combustion at 230 °C. The activities for HCHO and $CH_3OH$ oxidation increased with increasing manganese loadings.

Torres et al. [25] prepared mesoporous $MnO_x$ catalysts using the template-assisted method followed by an acidic treatment for the oxidation of formaldehyde. The structural, textural, and redox properties of $MnO_x$ catalysts were deeply modified when an acidic treatment was carried out after the calcination step. The specific surface area was increased by 75% and redox properties were promoted at low temperatures due to the oxidation of $Mn^{+3}$ to $Mn^{+4}$. As a result, the catalytic oxidation of formaldehyde took place at low temperatures.

The main objective of present work was to study the catalytic oxidation of formaldehyde, carbon monoxide, and methanol over the base metal oxides supported on cordierite monoliths calcined at high temperatures. The deactivation of base metal oxides by migrating $SiO_2$ from the cordierite to the active catalyst was presented and the effect of barrier coats composed of alkali-earth metal (Ba, Sr, Ca, Mg) oxides and alumina on the activities of base metal oxides for HCHO, CO, and $CH_3OH$ oxidation was investigated to develop the base metal oxides free of expensive platinum and rhodium precious metals supported on cordierite monoliths for methanol-fueled vehicles.

## EXPERIMENTAL

### 1. Catalyst Preparation

The base metal oxides (BMO) comprising 27% $MnO_2$, 21% $CeO_2$, and 52% $Al_2O_3$ were prepared by coprecipitation method. Saturated ammonium bicarbonate (Aldrich Co., 99.0%) was slowly added to an aqueous solution containing $Mn(NO_3)_2{\cdot}4H_2O$ (Aldrich Co., 99.0%), $Ce(NO_3)_3{\cdot}6H_2O$ (Aldrich Co., 99.0%), and $Al(NO_3)_3{\cdot}9H_2O$ (Aldrich Co., 98.0%) at 50 °C until the pH value of the mixture reached 6.9 with stirring and $CO_2$ sparging. The precipitate was further aged at 50 °C for 1 h in the mother liquid. After filtration and washing with distilled water several times, the obtained cake was dried at 120 °C for 24 h. A dried precipitate was calcined at 1,000 °C for 3 h in air to test the activities of base metal oxides in the condition of methanol-fueled vehicle operation. After calcination the base metal oxides were either screened to 8-14 mesh for granular catalysts, or milled for subsequent impregnation on a monolith. In the latter case, the material is milled wet in a ball mill with the 20% (or 14%) colloidal ceria for 24 h to improve the adherence of catalytic material to the support. The monolith support was coated by dipping the support into a slurry of the milled base metal oxides. The coated support was dried at 120 °C for 24 h and calcined at 1,000 °C for 3 h in air.

### 2. Activity Measurement

The reactions were carried out under an atmospheric pressure with a tubular flow reactor made of quartz tube (inner diameter 20 mm). Monolith sample was 35 mm by 14 mm OD and wrapped in a ceramic fiber paper to fit tight in the reactor. Granules were packed in small quartz cups with perforated bottoms. Ten milliliters of the catalysts was charged in the reactor and the reactor was heated with an electric furnace. $N_2$, $O_2$, CO, and $CO_2$ were supplied from individual gas cylinders. The flow rate of each gas was controlled by mass flow controller. Molecular sieve (10X) traps were installed in the $N_2$, $O_2$, and $CO_2$ supply lines. A carbonyl trap, packed with potassium carbonate impregnated on alumina ($K_2CO_3/Al_2O_3$) spheres, was installed to remove iron carbonyl.

Liquid components including formaldehyde, methanol, and water were fed into the evaporator by use of an automatically driven syringe under a flow of nitrogen. The vaporized mixture was then supplied to the reactor through a line electrically heated at 120 °C to avoid the condensation of the reagents. The feed gases passed downward through the reactor and sequentially contacted stacked layers of quartz bead, the catalyst, and quartz wool. Temperatures were measured with a chromel-alumel thermocouple positioned along the centerline with its tip located in the catalyst bed a few millimeters below the top of bed.

The composition of the reacting gas mixture was HCHO: 0.07%, $CH_3OH$: 0.5%, CO: 1.1%, $H_2O$: 17.6%, $CO_2$: 15.6%, $O_2$: 1.7%, and $N_2$: 63.2%. The space velocity of this reaction gas was 50,000 $h^{-1}$ unless otherwise noted. The reaction was carried out from room temperature to 500 °C with steps of 50 °C. $N_2$, $O_2$, and CO were analyzed by using a Hewlett Packard 5890 gas chromatograph using a molecular sieve 13X column and a thermal conductivity detector. HCHO, $CH_3OH$, and $CO_2$ were analyzed by using a Porapak-T column, a methanation column, and a flame ionization detector.

The BET surface areas were measured by the physical adsorption of nitrogen on the samples. $N_2$ adsorption isotherms of the samples were obtained at −196 °C using a Micromeritics ASAP 2010 instrument. The specific surface area was determined by using the linear portion of the Brunauer-Emmett-Teller (BET) model, and the average pore size was calculated by using the Barrett-Johner-Halenda (BJH) formula from the desorption branch of the $N_2$ adsorption isotherm. Before these measurements, the samples were degassed under vacuum at 350 °C for 24 h. X-ray powder diffraction (XRD) patterns were recorded with an Expert PRO MRD diffractometer (Phillips, U.S.A.) operated at 40 kV and 250 mA using nickel-filtered $CuK_\alpha$ ($\lambda$=1.5406 Å) radiation.

## RESULTS AND DISCUSSION

Fig. 1 shows steady-state conversions for HCHO (solid curve), CO (dash curve), and $CH_3OH$ (dash-dot curve) oxidation as a function of catalyst temperature over base metal oxides (BMO) comprising 27% $MnO_2$, 21% $CeO_2$, and 52% $Al_2O_3$ in a granular form calcined at 1,000 °C for 3 h in air. The BMO catalyst initiated the

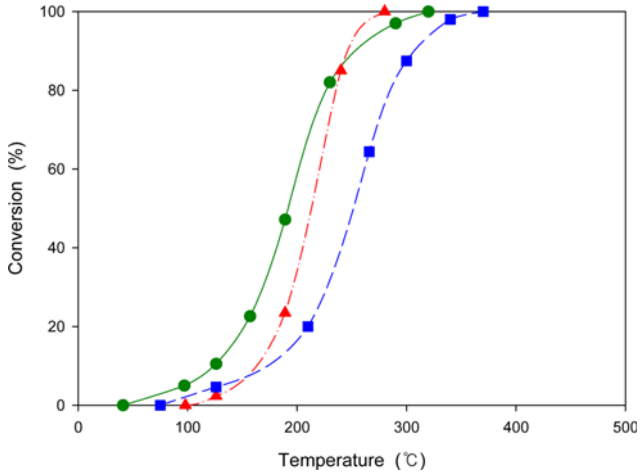


**Fig. 1. Conversion versus temperature profiles for HCHO (—●—), CO (--■--), and $CH_3OH$ (--▲--) oxidation over the granular BMO catalyst calcined at 1,000 °C for 3 h in air.**

oxidation of HCHO, CO, and $CH_3OH$ at 40, 75, and 100 °C and reached the complete conversion of HCHO, CO, and $CH_3OH$ at 320, 370, and 280 °C, respectively.

Formaldehyde oxidized more readily over the BMO catalyst in a granular form calcined at 1,000 °C for 3 h in air. Carbon monoxide oxidized more difficultly over the BMO catalyst. The activity of the BMO catalyst for methanol oxidation was placed between the formaldehyde and carbon monoxide oxidation. The activities of the BMO catalyst in the granular form calcined at 1,000 °C for 3 h in air for the oxidation of formaldehyde were higher than those for the oxidation of methanol at the temperature below 240 °C. Above 240 °C the activities of the BMO catalyst for the oxidation of methanol were higher than those for the oxidation of formaldehyde. The conversion versus temperature profile for HCHO oxidation is similar to that for CO oxidation. $CO_2$ and $H_2O$ were the only products of HCHO oxidation observed in this study. Steady-state conversions for HCHO, CO, and $CH_3OH$ oxidation over the commercial precious metal catalyst (0.5% $Pt/Al_2O_3$) calcined at 1,000 °C for 3 h in air are shown in Fig. 2. The precious metal catalyst initiated the oxidation of HCHO, CO, and $CH_3OH$ equally at 235 °C and approached the complete conversion of HCHO, CO, and $CH_3OH$ equally at 240 °C, respectively.

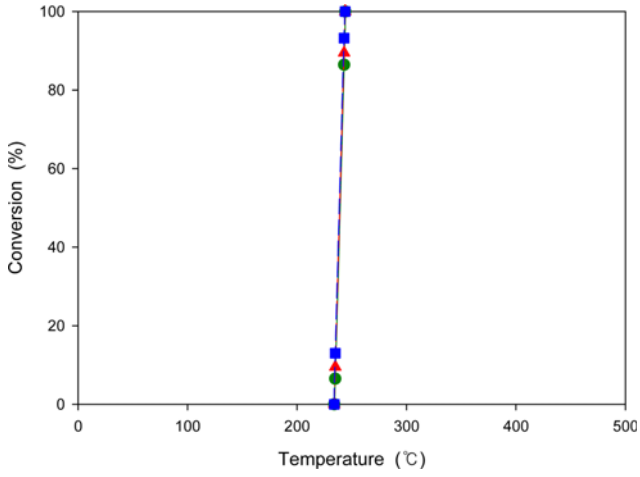


**Fig. 2. Conversion versus temperature profiles for HCHO (—●—), CO (--■--), and $CH_3OH$ (--▲--) oxidation over 0.5 wt% Pt supported on 0.32 cm alumina sphere calcined at 1,000 °C for 3 h in air.**

McCabe and McCready [15] studied the formaldehyde oxidation on a Pt wire. They found that the kinetics of the Pt-catalyzed oxidation of formaldehyde was similar to carbon monoxide oxidation kinetics. The dissociative adsorption as CO(a) and H(a) was followed by surface reaction with O(a) to produce $CO_2$(g) and $H_2O$ (g). The low-temperature regime is characterized by high concentration of CO(a) which inhibits $O_2$ adsorption, thereby resulting in negative-order CO and positive-order $O_2$ kinetics. As the temperature is increased, the CO desorption rate increases sharply due to the high activation energy for CO desorption. Thus, the concentration of CO(a) decreases at high temperatures allowing rapid adsorption and reaction of oxygen.

The activity of the BMO catalyst for HCHO oxidation was much higher than that of the precious metal catalyst at the temperatures below 200 °C as shown in Figs. 1-2. The conversion versus temperature profile for $CH_3OH$ oxidation over the BMO catalyst shifted to a little higher temperature for the precious metal catalyst. Conversely, the activity of the precious metal catalyst for CO oxidation was higher than that of the BMO catalyst. It is noted that the conversion for HCHO, CO, and $CH_3OH$ oxidation over the precious metal catalyst calcined at 1,000 °C for 3 h in air increased very rapidly near 235 °C as depicted in Fig. 2. The light-off temperature ($T_{50\%}$) of the precious metal catalyst calcined at 1,000 °C for 3 h in air for HCHO oxidation was marginally 50 °C higher than that of the BMO catalysts as shown in Table 1.

Cordierite ($2MgO{\cdot}3Al_2O_3{\cdot}5SiO_2$) is widely used as a support in the present three-way catalyst to remove CO, HC, and $NO_X$ emitted from gasoline-fueled vehicles. Cordierite has the property of high resistance to thermal shock, which is attributable to its high silica content. Therefore, cordierite may not be suitable without major modification as a support for the BMO catalyst to remove the HCHO, CO, and $CH_3OH$ emitted from methanol-fueled vehicles. The activities of the BMO catalyst supported on cordierite monoliths (64 cells/$cm^2$) calcined at 1,000 °C for 3 h in air dropped off drastically, that was different from the BMO catalyst in granular form calcined at 1,000 °C for 3 h in air.

To determine why the activity of the cordierite-supported BMO catalyst lost after calcination at 1,000 °C for 3 h in air, we conducted two kinds of experiment using the cordierite monoliths (EX-20) as the supports for methanol-fueled vehicles. First, a cordierite support

**Table 1. Light-off temperatures of the granular BMO and precious metal catalysts calcined at 1,000 °C for 3 h in air**

| Catalyst | Shape | Calcination temperature (°C) | Light-off temperature (°C) for HCHO oxidation | | |
|---|---|---|---|---|---|
| | | | $T_{10\%}$ | $T_{50\%}$ | $T_{90\%}$ |
| BMO | Granular | 1,000 | 110 | 190 | 240 |
| PM | Granular | 1,000 | 235 | 240 | 245 |

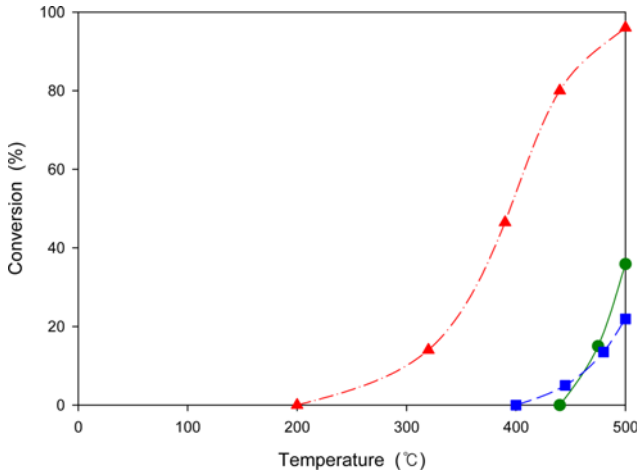


**Fig. 3. Conversion versus temperature profiles for HCHO (—●—), CO (--■--), and $CH_3OH$ (---▲---) oxidation over the 49.0% BMO catalyst supported on the cordierite monolith (EX-20) calcined at 1,000 °C for 3 h in air.**

was coated with the 49% BMO catalyst, which was thick enough to form a thickness as great as the webs of the cordierite. Despite the high loading of base metal oxides, the activity of cordierite-supported catalyst turned out to be very poor, as shown in Fig. 3. The activity of the BMO catalyst supported on cordierite monolith calcined at 1,000 °C for 3 h in air initiated the oxidation of HCHO at 440 °C and CO at 400 °C much higher than that of the BMO catalyst in a granular form calcined at 1,000 °C for 3 h in air (see Fig. 1). Therefore, the loss in activity was not due to the catalyst migration into and being blocked from contact with the gas by the support.

Second, one sample was loaded with the 27.6% BMO catalyst on the $\gamma$-$Al_2O_3$ monolith obtained from Corning. The other sample was coated first with colloidal silica and then with the 26.2% BMO catalyst on the $\gamma$-$Al_2O_3$ monolith. The activity of $\gamma$-$Al_2O_3$-supported BMO catalysts with and without the silica for the oxidation of HCHO, CO, and $CH_3OH$ was compared for identifying the $SiO_2$ migration from the cordierite to the BMO catalyst. The better activity of $\gamma$-$Al_2O_3$-supported BMO catalyst for HCHO, CO, and $CH_3OH$ oxidation was obtained in the absence of silica as shown in Fig. 4. A mobile silica from the cordierite to the base metal oxides was deactivating the supported catalyst. The loss of catalytic activity during the high temperature calcination at 1,000 °C is the presence of loosely bound silica in the monolith support that migrates to the surface during calcination and reacts with or physically block the active catalyst.

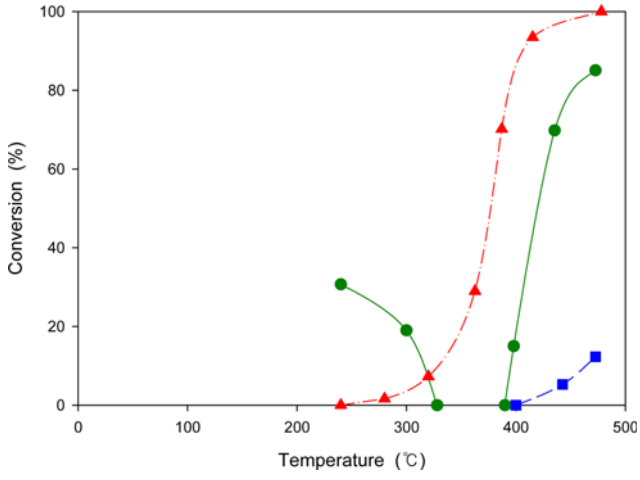


**Fig. 4. Conversion versus temperature profiles for HCHO (—●—), CO (--■--), and $CH_3OH$ (---▲---) oxidation over the 27.6% BMO catalyst supported on the $\gamma$-$Al_2O_3$ monolith obtained from Corning and calcined at 1,000 °C for 3 h in air.**

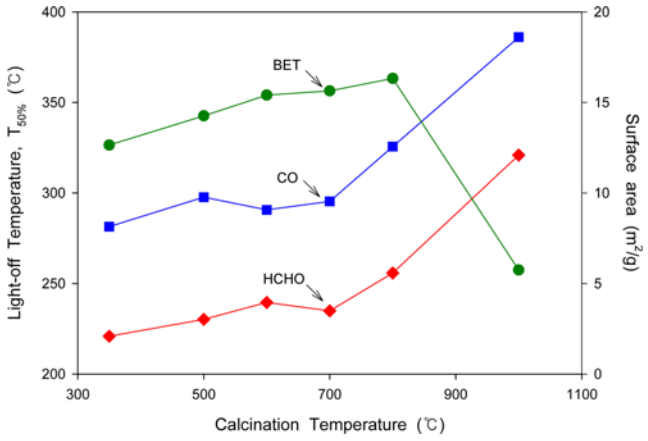


**Fig. 5. Effect of calcination temperature on the light-off temperatures for HCHO (—●—) and CO (--■--) oxidation and surface area over the BMO catalysts supported on cordierite monolith (EX-20) calcined at 1,000 °C for 3 h in air.**

To find the cause of activity loss on the BMO catalyst supported on the cordierite monolith calcined at 1,000 °C for 3 h in air, the light-off temperatures ($T_{50\%}$) for HCHO and CO oxidation over the cordierite-supported BMO catalysts calcined at the temperatures between 350 and 1,000 °C for 3 h in air were plotted in Fig. 5. The light-off temperatures of cordierite-supported BMO catalysts for both HCHO and CO oxidation increased with the increasing calcination temperature. The rate of the change in the light-off temperatures was lower below 700 °C while its change rate was higher above 700 °C. The change rate below 700 °C turned out to be 0.03%/°C while its change rate above 700 °C was equal to 0.3%/°C.

The BET surface areas of the cordierite-supported BMO catalysts calcined at different temperatures between 350 and 1,000 °C were also measured by nitrogen adsorption. The BET surface area increased with the increasing calcination temperature below 800 °C. But the BET surface area decreased very rapidly from 16.3 $m^2/g$ at 800 °C to 5.7 $m^2/g$ at 1,000 °C with the rate of 0.05 $m^2/g$·°C above 800 °C. The deactivation of the cordierite-supported BMO catalyst started with the calcination temperature between 700 and 800 °C. Its effect was quite significant for the BMO catalyst supported on a cordierite monolith after calcination at 1,000 °C for 3 h in air. The increase of BET surface areas with the increasing calcination temperatures below 800 °C might occur due to the creation of a network of submicroscopic cracks and crevices resulting from the density change together with the dehydroxylation of the alumina.

To understand the decrease of surface area above the temperature between 700 and 800 °C, the pore size distribution of the cord-

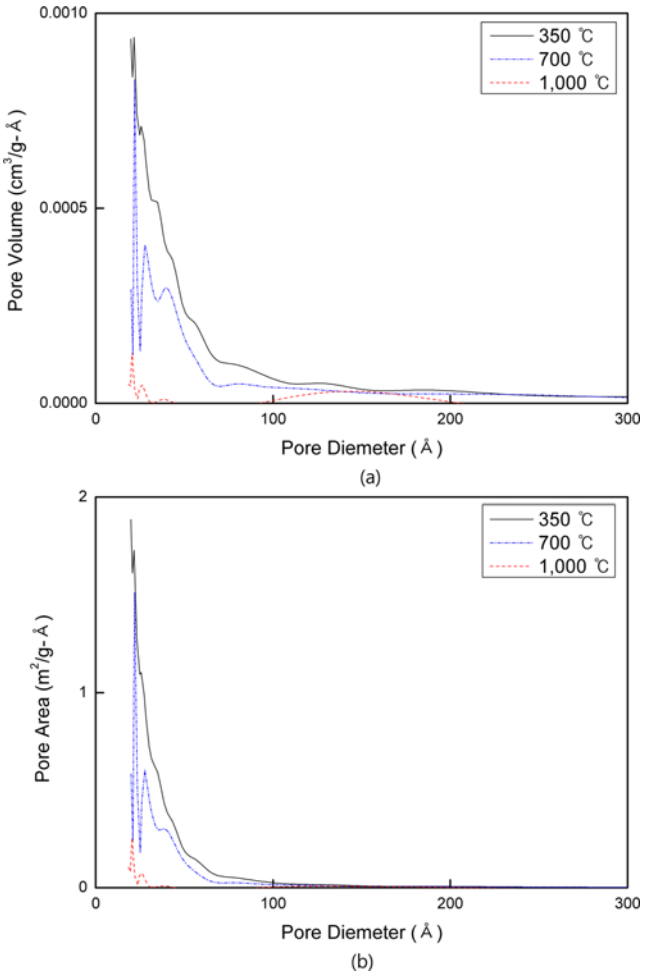


**Fig. 6. Pore size distribution of the cordierite-supported BMO catalysts calcined at 350 °C (———), 700 °C (—.—), and 1,000 °C (——) for 3 h in air in terms of pore volume (a) and surface area (b).**

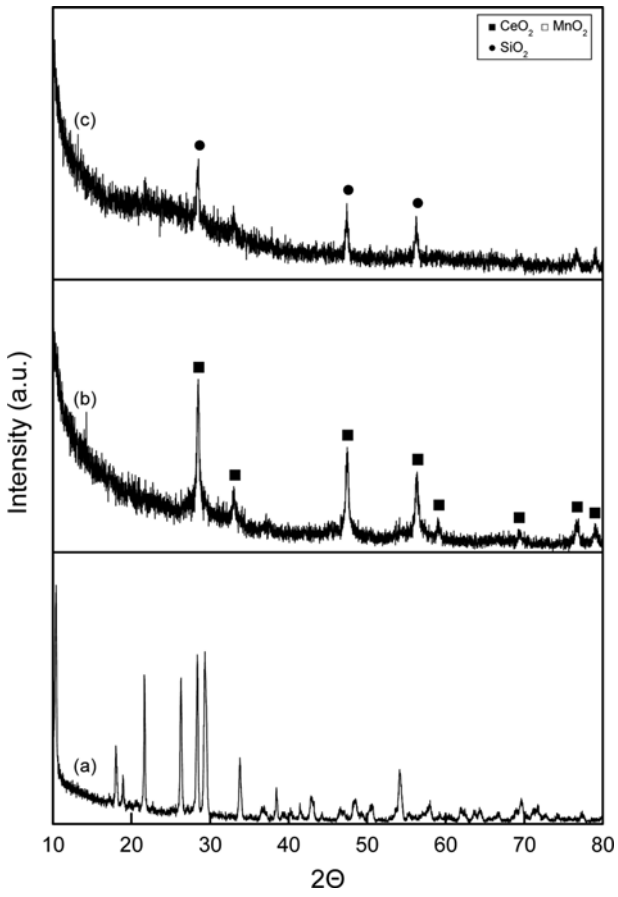


**Fig. 7. XRD patterns of the cordierite (a) and the cordierite-supported BMO catalysts calcined at 350 °C (b) and 1,000 °C (c) for 3 h in air.**

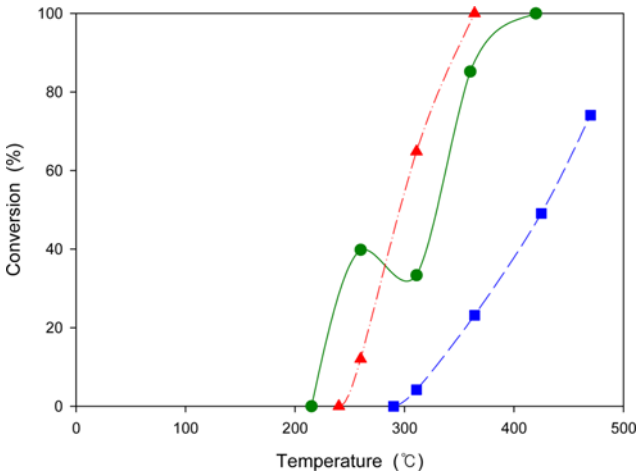


**Fig. 8. Conversion versus temperature profiles for HCHO (—●—), CO (--■--), and $CH_3OH$ (--▲--) oxidation over the 14.4% BMO catalyst supported on cordierite monolith (EX-20) calcined at 700 °C for 3 h in air.**

ierite-supported BMO catalysts calcined at 350, 700, and 1,000 °C for 3 h in air was measured by using nitrogen desorption as shown in Fig. 6. As can be seen, the pore volume of the cordierite-supported BMO catalysts calcined at 700 and 1,000 °C for 3 h in air decreased by 42% and 90% compared with that of the cordierite-supported BMO catalyst calcined at 350 °C for 3 h in air, respectively, suggesting that the sintering of base metal oxides supported on the cordierite or the $SiO_2$ migrated from the cordierite to the BMO catalyst plugs the pores of the BMO catalyst. The surface area of the cordierite-supported BMO catalysts calcined at 700 and 1,000 °C for 3 h in air decreased by 63% and 94% compared with that of the cordierite-supported BMO catalyst calcined at 350 °C for 3 h in air similar to the decrease of the pore volume of the cordierite-supported BMO catalysts calcined at higher temperatures.

XRD patterns of the base metal oxides supported on the cordierite and calcined at 350 and 1,000 °C are shown in Fig. 7. All of the BMO catalysts were crystallized as indicated by the sharp peaks for $CeO_2$, $MnO_2$, and $SiO_2$. All the major peaks were found to match the standard peaks of $CeO_2$ (JCPDS card number 34-0394), $MnO_2$ (JCPDS card number 24-0735), and $SiO_2$ (JCPDS card number 33-1161). Most of peaks for $MnO_2$ overlapped with those of $CeO_2$. The strongest peak of $SiO_2$ at $2\theta$=26.6° indicates the existence of $SiO_2$ migrated from the cordierite to base metal oxides.

Fig. 8 shows steady-state conversions for HCHO, CO, and $CH_3OH$ oxidation as a function of catalyst temperature over the cordierite-supported BMO catalyst calcined at 700 °C for 3 h in air. This catalyst initiated the oxidation of HCHO, CO, and $CH_3OH$ at 210, 290, and 230 °C, respectively. An unusual conversion versus temperature profile was obtained for HCHO oxidation differently from those for CO and $CH_3OH$ oxidation. The HCHO conversion increased with temperature to a level near 38% at 260 °C, then decreased precipitously to a level near 32% at 310 °C. At higher temperatures the conversion again increased to high level. The decrease of the conversion for HCHO oxidation may arise from the partial oxidation or dehydrogenation of $CH_3OH$ as shown in Eqs. (1) and (2). It is noted that the conversion for HCHO oxidation decreased shortly after the conversion for $CH_3OH$ oxidation started to rise as shown in Fig. 8. After the oxidation of $CH_3OH$ took place at an inflection point, the conversion for HCHO oxidation again increased with the increasing temperature.

$$CH_3OH+1/2\ O_2 \rightarrow HCHO+H_2O \qquad \Delta H^o=-149.7\ kJ/mol \qquad (1)$$

$$CH_3OH \rightarrow HCHO+H_2 \qquad \Delta H^o=92.0\ kJ/mol \qquad (2)$$

The conversion versus temperature profiles of saddle type for HCHO oxidation over the cordierite-supported BMO catalysts were also detected in Figs. 3-4. McCabe and Mitchell [14] reported that unusual behavior was observed with the Pd catalyst, which showed local minima in the HCHO conversion versus temperature profiles. These saddles were similar to, but more pronounced than, those in $CH_3OH$ oxidation. The depths of saddles in the HCHO and $CH_3OH$ conversion profiles correlated with the feed equivalence ratio, with the deepest saddles occurring in feeds containing a large excess of $O_2$. But they didn't observe the HCHO conversion versus temperature profile of saddle type over the 4% Cu-2% Cr base metal oxides. Their calcination temperature at 500 °C was different from our calcination temperature at 1,000 °C.

The effect of silica on precious metal catalyst activities had been examined in several studies. Gentry and Jones [26] studied the deactivation of adding hexamethyldisiloxane (HMDS) on the oxidation of $CH_4$, $C_3H_6$, CO, and $H_2$ over the Pt/$\gamma$-$Al_2O_3$ catalyst in detail. The oxidation rate of $H_2$ at 600 °C was negligibly affected by the presence of HMDS. In contrast the rates of $CH_4$ and $C_3H_6$ oxidation at 600 °C were significantly reduced. With the removal of HMDS from the inlet gas, the rate of $C_3H_6$ oxidation recovered nearly completely. In contrast $CH_4$ oxidation did not recover, leading these investigators to propose that each of the reactions occurred over different active sites. They also found that silicon atoms from the organosilicon compounds physically block active surface sites.

The deactivation of precious metal ozone decomposition catalyst had been attributed to the presence of silica, phosphorus, and sulfur in the aged catalyst [27,28]. The cyclohexane dehydrogenation reaction was studied over palladium black on which triethylsilane was decomposed at 250 °C [29]. Using XPS characterization of the catalyst, they proposed that silica coats the surface and diffuses into bulk palladium, thereby detrimentally impacting hydrogenation activity. Oxidation restores hydrogenation activity by converting surface silicon to silica, which is either permeable to hydrogen or exists as islands on the palladium.

The deactivation of Pt and Pd catalysts supported on $\gamma$-$Al_2O_3$ beads by silica was studied in a flexographic printing application [30]. Organosilicon compounds contained in the printing ink diffuse into the catalyst and deposit as silica particles in the micropores. Activity evaluation of aged catalysts suggests that silica deposition is non-selective and that silica masks metal active site.

To immobilize migrating $SiO_2$ from the cordierite to the base metal oxides to react or physically block the active catalyst, alkali-earth metal oxides coprecipitated with alumina were used as the barrier coats. Coated materials with one to one atomic ratios of alkali-earth metal to aluminum have been prepared from barium, strontium, calcium, and magnesium. Each material has been impregnated onto the cordierite monolith and subsequently coated with the base metal oxides. The light-off temperatures ($T_{50\%}$) of the cordierite-supported BMO catalysts pretreated with barrier coats and calcined at 1,000 °C for 3 h in air are summarized in Table 2. The light-off temperatures ($T_{50\%}$) of the cordierite-supported BMO catalysts pretreated with the BaO-$Al_2O_3$, CaO-$Al_2O_3$, SrO-$Al_2O_3$, and MgO-$Al_2O_3$ barrier coats and calcined at 1,000 °C for 3 h in air were observed at 235, 250, 335, and 375 °C for the oxidation of formaldehyde as shown in Table 2. The presence of a barrier coat containing either barium or calcium reduced the deactivation otherwise observed when the cordierite-supported BMO catalyst was calcined at 1,000 °C for 3 h in air. The best activity was obtained with the BaO-$Al_2O_3$ barrier coat as shown in Table 2. Fig. 9 shows the activities of the 24.3% BMO catalyst supported on the cordierite pretreated with the 15.0% MgO-$Al_2O_3$ barrier coat and calcined at 1,000 °C for 3 h in air. Clearly, the activities of the cordierite-supported BMO catalyst pretreated with the MgO-$Al_2O_3$ barrier coat were much improved compared with those of the cordierite-supported BMO catalyst (see Fig. 4).

To find the optimum composition of the BaO-$Al_2O_3$ barrier coat,

**Table 2. Effect of barrier coats on the light-off temperatures for the oxidation of HCHO, CO, and $CH_3OH$ over the cordierite-supported BMO catalysts**

| Catalyst | Support | Barrier coat | Calcination temperature (°C) | Light-off temperature, $T_{50\%}$ (°C) | | |
|---|---|---|---|---|---|---|
| | | | | HCHO | CO | $CH_3OH$ |
| BMO | Cordierite | None | 1,000 | 320 | 390 | 290 |
| BMO | Cordierite | BaO-$Al_2O_3$ | 1,000 | 235 | 270 | 260 |
| BMO | Cordierite | CaO-$Al_2O_3$ | 1,000 | 250 | 345 | 260 |
| BMO | Cordierite | SrO-$Al_2O_3$ | 1,000 | 335 | 400 | 290 |
| BMO | Cordierite | MgO-$Al_2O_3$ | 1,000 | 375 | 510 | 318 |

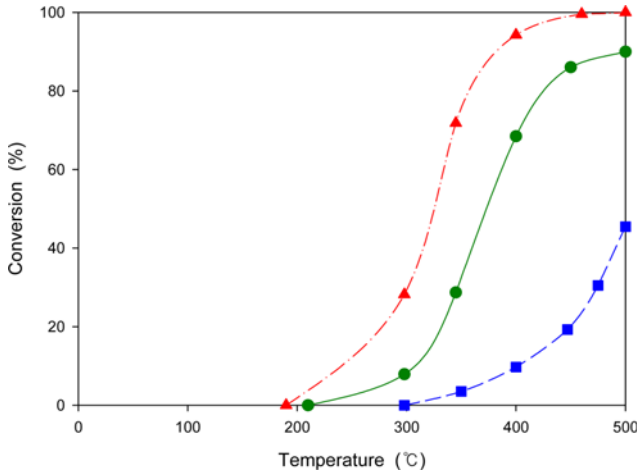


**Fig. 9. Conversion versus temperature profiles for HCHO (—●—), CO (--■--), and $CH_3OH$ (--▲--) oxidation over the 24.3% BMO catalyst pretreated with the 15.0% MgO-$Al_2O_3$ barrier coat and calcined at 1,000 °C for 3 h in air.**

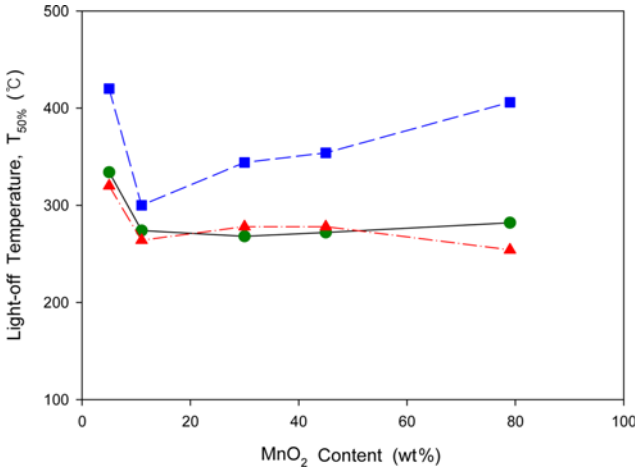


**Fig. 11. Effect of the $MnO_2$ content in the granular BMO catalyst on the light-off temperatures ($T_{50\%}$) for HCHO (—●—), CO (--■--), and $CH_3OH$ (--▲--) calcined at 1,000 °C for 3 h in air.**

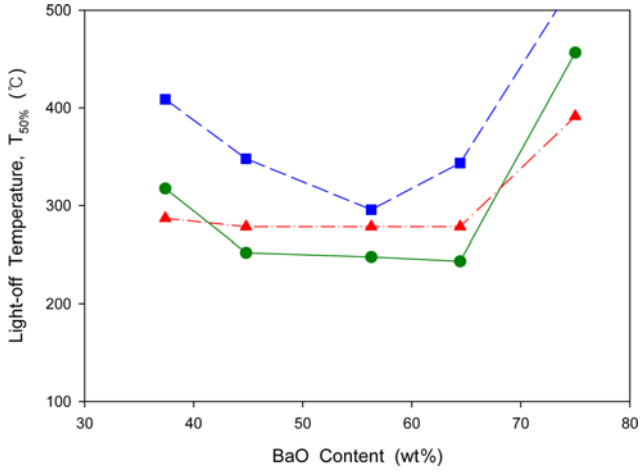


**Fig. 10. Effect of the BaO content in the BaO-$Al_2O_3$ barrier coat over the BMO catalyst supported on cordierite monolith (EX-20) calcined at 1,000 °C for 3 h in air on the light-off temperatures for HCHO (—●—), CO (--■--), and $CH_3OH$ (--▲--) oxidation.**

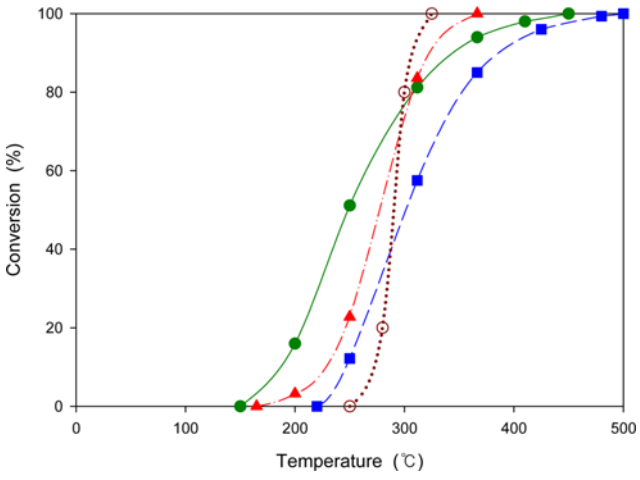


**Fig. 12. Conversion versus temperature profiles for HCHO (—●—), CO (--■--), and $CH_3OH$ (--▲--) oxidation over the cordierite-supported BMO catalyst pretreated with the BaO-$Al_2O_3$ barrier coat and calcined at 1,000 °C for 3 h in air. Dotted line represents the conversion for HCHO, $CH_3OH$, and CO oxidation over the 0.5% Pt supported on 0.32 cm alumina sphere.**

the light-off temperatures ($T_{50\%}$) of the cordierite-supported BMO catalyst pretreated with the 22.1% BaO-$Al_2O_3$ barrier coats, with the BaO content ranging from 35 to 75% are shown in Fig. 10. The light-off temperatures ($T_{50\%}$) for HCHO and $CH_3OH$ oxidation changed smoothly when 45 to 66% BaO content was used in the BaO-$Al_2O_3$ barrier coats. The light-off temperature for CO oxidation changed more rapidly. Methanol oxidation did not appear to be sensitive to the content of BaO below 66% in the BaO-$Al_2O_3$ barrier coats. The minimum light-off temperatures for the HCHO and $CH_3OH$ oxidation occurred at the BaO content of 66%. This corresponds to a one-to-one atomic ratio of barium to aluminum.

To investigate the optimum concentration of manganese dioxide in the BMO catalysts $MnO_2$ concentration was varied from 5.0 to 80.0% while holding the atomic ratio of aluminum to cerium constant. The light-off temperatures of the BMO catalysts in a granular form calcined at 1,000 °C for 3 h in air are depicted in Fig. 11. The activity of the BMO catalysts for the oxidation of CO was very sensitive to the $MnO_2$ concentration. HCHO and $CH_3OH$ oxidation was comparatively insensitive to the $MnO_2$ concentration. The best performance of the BMO catalysts for the oxidation of HCHO was obtained with the composition containing 30.0% $MnO_2$. Therefore, the $MnO_2$ concentration in the BMO catalysts studied in this work was very close to the optimum $MnO_2$ concentration.

Fig. 12 shows steady-state conversions for HCHO, CO, and $CH_3OH$ oxidation as a function of catalyst temperature over the 22.1% BMO catalyst supported on the cordierite monolith pretreated with the 66% BaO-$Al_2O_3$ barrier coat and calcined at 1,000 °C for

3 h in air. Also shown are the corresponding oxidation curves over the 0.5% Pt supported on $Al_2O_3$ beads calcined at 1,000 °C for 3 h in air. The cordierite-supported BMO catalyst pretreated with the 66% BaO-$Al_2O_3$ barrier coat initiated the oxidation of HCHO, CO, and $CH_3OH$ at 150, 220, and 170 °C, respectively. The cordierite-supported BMO catalyst showed better activity than the 0.5% Pt/$Al_2O_3$ precious metal catalyst at temperatures below 280 °C. Formaldehyde oxidized more readily over the cordierite-supported BMO catalyst below 300 °C. But above 300 °C methanol oxidized more readily over the cordierite-supported BMO catalyst. Carbon monoxide oxidized more difficultly over the cordierite-supported BMO catalyst.

To improve the activity of the cordierite-supported BMO catalyst pretreated with the 66% BaO-$Al_2O_3$ barrier coat and calcined at 1,000 °C for 3 h in air, the palladium with no Pt or Rh was incorporated into the cordierite-supported BMO catalyst. The palladium loading was varied from 0.00057 to 0.147% to the cordierite-supported BMO catalyst. Their activities for HCHO, CO, and $CH_3OH$ oxidation are shown in Fig. 13. Their light-off temperatures ($T_{50\%}$) for HCHO, CO, and $CH_3OH$ oxidation are summarized in Table 3. The light-off temperatures ($T_{50\%}$) for the commercial precious metal catalyst supported on the $Al_2O_3$ beads are also shown for comparison. At the higher loading (0.147% Pd) the palladium-incorporated BMO catalyst outperformed the precious metal catalyst as shown in Fig. 13. The light-off temperature curves of the cordierite-supported BMO catalyst pretreated with the 66% BaO-$Al_2O_3$ barrier coat and calcined at 1,000 °C for 3 h in air for HCHO, CO, and $CH_3OH$ oxidation were sharp and occurred at lower temperatures between 220 and 230 °C. The temperatures of 50% conversion of HCHO, CO, and $CH_3OH$ oxidation were 70 °C lower over base metal oxides catalyst than over precious metal catalyst. The conversion versus temperature profiles of saddle type for HCHO oxidation resulting from the partial oxidation or dehydrogenation of the methanol were not observed with the palladium-incorporated BMO catalyst.

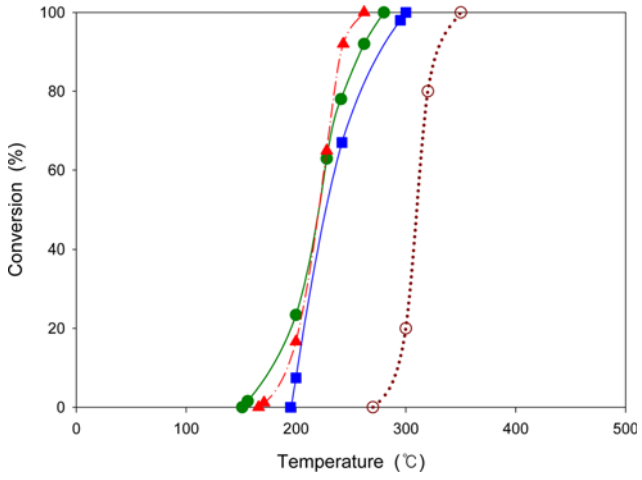


**Fig. 13. Conversion versus temperature profiles for HCHO (—●—), CO (--■--), and $CH_3OH$ (--▲--) oxidation over the cordierite-supported BMO catalyst with the incorporation of 0.147% Pd pretreated with the BaO-$Al_2O_3$ barrier coat and calcined at 1,000 °C for 3 h in air. Dotted line represents the conversion for HCHO, $CH_3OH$, and CO oxidation over the 0.5% Pt supported on 0.32 cm alumina sphere.**

## CONCLUSIONS

The base metal oxide (BMO) catalyst in a granular form calcined at 1,000 °C for 3 h in air was active for the oxidation of formaldehyde, carbon monoxide, and methanol. But the activity of the BMO catalyst supported on the cordierite monolith calcined at 1,000 °C for 3 h in air was greatly suppressed due to the migration of mobile silica from the cordierite to the base metal oxides to react with or physically block the active catalyst. To immobilize the migrating silica, barrier coats composed of alkali-earth metal oxides and alumina were examined and the best activity was obtained with the 66% BaO-$Al_2O_3$ barrier coat.

The cordierite-supported BMO catalyst pretreated with the 66% BaO-$Al_2O_3$ barrier coat and calcined at 1,000 °C for 3 h in air initiated the oxidation of formaldehyde, carbon monoxide, and methanol at 150, 220, and 170 °C, respectively. This catalyst showed better activity for the formaldehyde oxidation than the 0.5 Pt/$Al_2O_3$ precious metal catalyst below 280 °C. The incorporation of a small amount of palladium (0.147% Pd) to the cordierite-supported BMO catalyst pretreated with the 66% BaO-$Al_2O_3$ barrier coat and calcined at 1,000 °C for 3 h in air improved the activity for the oxidation of formaldehyde, carbon monoxide, and methanol. The conversion versus temperature profiles for formaldehyde, carbon monoxide, and methanol turned out to be sharp and they occurred at lower temperatures between 150 and 200 °C. The temperatures of 50% conversion of formaldehyde, carbon monoxide, and methanol were 70 °C lower over base metal oxides catalyst than over precious metal catalyst. The conversion versus temperature profiles of saddle type for HCHO oxidation resulting from the partial oxidation or dehy-

**Table 3. Light-off temperatures of the Pd-incorporated BMO catalysts supported on cordierite monoliths pretreated with BaO-$Al_2O_3$ barrier coats and calcined at 1,000 °C for 3 h in air**

| Catalyst | Support | Barrier coat | Pd loading (wt%) | Light-off temperature, $T_{50\%}$ (°C) | | |
|---|---|---|---|---|---|---|
| | | | | HCHO | CO | $CH_3OH$ |
| BMO | Cordierite | BaO-$Al_2O_3$ | 0.147 | 220 | 228 | 222 |
| BMO | Cordierite | BaO-$Al_2O_3$ | 0.0147 | 321 | 307 | 285 |
| BMO | Cordierite | BaO-$Al_2O_3$ | 0.0028 | 243 | 310 | 260 |
| BMO | Cordierite | BaO-$Al_2O_3$ | 0.000576 | 352 | 440 | 316 |
| PM | Alumina | None | 0.5% Pt | 302 | 291 | 292 |

drogenation of the methanol were not observed with the palladium-incorporated BMO catalyst. The long stability and poison resistance of the palladium-incorporated BMO catalyst supported on the cordierite monolith shall be investigated in the next study.

## ACKNOWLEDGEMENT

This work was supported by the Konkuk University in 2010. We wish to thank Dr. A. Stiles for suggesting preparative methods for the laboratory-prepared catalysts.

## REFERENCES

1. H. G. Adelman, D. G. Andrews and R. S. Devoto, *SAE Paper* **720693** (1972).
2. G. K. Piotrowski and J. D. Murrell, *SAE Paper* **872052** (1987).
3. R. J. Nichols, E. L. Clinton, E. T. King, C. S. Smith and R. J. Wineland, *SAE Paper* **881200** (1988).
4. J. C. Summers, J. J. White and W. B. Williamson, *SAE Paper* **890794** (1989).
5. F. P. Jakse, R. M. Friedman, F. S. Delk and J. W. Buloch, *Appl. Catal.*, **14**, 303 (1985).
6. D. Sodhi, M. A. Abraham and J. C. Summers, *J. Air Waste Manage. Assoc.,* **40**, 352 (1990).
7. K. T. Chuang, B. Zhou and S. Tong, *IEC Res.*, **33**, 1680 (1994).
8. A. Nishimura and Y. Sekine, *Atmos. Environ.*, **35**, 2001 (2001).
9. Y. Sekine, *Atmos. Environ.*, **36**, 5543 (2002).
10. C. Zhang, H. He and K. Tanaka, *Catal. Commun.*, **6**, 211 (2005).
11. X. Tang, Y. Li, X. Huang, Y. Xu, H. Zhu, J. Wang and W. Shen, *Appl. Catal. B: Environ.*, **62**, 265 (2006).
12. J. Peng and S. Wang, *App. Catal. B: Environ.*, **73**, 282 (2007).
13. R. W. McCabe and P. J. Mitchell, *IEC Prod. Res. Dev.*, **22**, 212 (1983).
14. R. W. McCabe and P. J. Mitchell, *IEC Prod. Res. Dev.*, **23**, 196 (1984).
15. R. W. McCabe and D. F. McCready, *Chem. Phys. Lett.*, **111**, 89 (1984).
16. R. W. McCabe and P. J. Mitchell, *Appl. Catal.*, **27**, 83 (1986).
17. R. W. McCabe and P. J. Mitchell, *J. Catal.*, **103**, 419 (1987).
18. R. W. McCabe and P. J. Mitchell, *Appl. Catal.*, **44**, 73 (1988).
19. J. J. Foster and R. I. Masel, *IEC Prod. Rev. Dev.*, **25**, 563 (1988).
20. S. Imamura, Y. Uematsu and K. Utani, *IEC Res.*, **30**, 18 (1991).
21. S. Imamura, D. Uchihori and K. Utani, *Catal. Lett.*, **24**, 377 (1994).
22. C. F. Mao and M. A. Vannice, *J. Catal.*, **154**, 230 (1995).
23. M. C. Alvarez-Galvan, B. Pawelec, V. A. O'shea, J. L. G. Fierro, and P. L. Arias, *Appl. Catal. B: Environ.*, **51**, 83 (2004).
24. V. A. O'shea, M. C. Alvarez-Galvan, J. L. G. Fierro and P. L. Arias, *Appl. Catal. B: Environ.*, **57**, 191 (2005).
25. J. Q. Torres, J.-M. Giraudin and J.-F. Lamonier, *Catal. Today*, **176**, 277 (2011).
26. S. J. Gentry and A. Jones, *J. Appl. Chem. Biotechnol.*, **28**, 727 (1978).
27. H. Gandhi, W. B. Williamson, R. L. Goss, L. D. Marcotty and D. Lewis, *SAE Paper* **860565** (1986).
28. R. M. Heck, R. J. Farauto and H. C. Lee, *Catal. Today,* **13**, 43 (1992).
29. G. V. Smith, J. Stochs, S. Degendra and T. Wiltowski, *Catal. Org. React.*, E. Pasco Ed., *Catalysis of organic reactions*, E. Pasco Ed., Marcel Dekker (1991).
30. C. Libanati, D. A. Ullenius and C. J. Pereira, *Appl. Catal. B: Environ.*, **15**, 21 (1998).